垂直細長空心圓柱之壁熱傳導與混合熱對流之共軛熱傳分析

Conjugated Heat Transfer Analysis of Wall Conduction and Mixed Convection Along Vertical Slender Hollow Cylinders

王添益

Tian-Yih Wang

摘要

透過考慮在牆壁熱傳導和混合對流之間的相互作用，本文對於牛頓流體沿著一個垂直細長中空之圓柱的共軛熱傳特性提出分析。文中提出了利用共軛熱傳參數作為控制指標，以顯示牆壁熱傳導的影響。座標和應變數作了轉換以得到一有效率的數值解。有關共軛熱傳參數、浮力參數、曲率參數和普朗特數對於流場和熱場之影響將被深入探討。

關鍵詞：牆壁熱傳導、混合對流、共軛熱傳參數、、浮力參數、曲率參數、普朗特數

ABSTRACT

By considering the interaction between wall conduction and mixed convection, an analysis is presented to study the conjugate heat transfer characteristics of Newtonian fluids along a vertical slender hollow cylinder. This paper proposes the use of a conjugate heat transfer parameter as control indicators to show the impact of the wall heat conduction. The coordinates and dependent variables are transformed to yield computationally efficient numerical solutions. The effects of the conjugate heat transfer parameter, the buoyancy parameter, the curvature parameter and the Prandtl number on the fluid fields and the thermal fields will be explored in depth.

Keywords：wall conduction, mixed convection, conjugated heat transfer parameter, buoyancy parameter, curvature parameter, Prandtl number

1. INTRODUCTION

The mixed convection flow along a cylinder is commonly found in several industrial and technical applications such as nuclear reactors, heat exchangers, pipe insulation systems, etc. For a slender cylinder, the radius of the cylinder may be the same order as the boundary layer thickness. Therefore, the flow must be considered symmetric and the governing equations should contain the transverse curvature term which strongly influences both the velocity and temperature fields and hence the corresponding skin friction coefficient and heat transfer rate at the wall.

The buoyancy and transverse curvature effects on forced convection of Newtonian fluids flow over a vertical cylinder have been analyzed by Chen and Mucoglu [1], Mucoglu and Chen [2], Bui and Cebeci [3], and Lee et al. [4, 5]. Wang and Kleinstreuer [6] used new mixed-convection parameters and conducted a general analysis of fluid flow and heat transfer for steady laminar mixed convection on vertical slender cylinders covering the

王添益　明志科技大學機械工程系副教授

entire range from forced convection to free convection. Recently, Kumari and Nath [7] presented the analysis of the effects of localized cooling/heating and injection/suction on the mixed convection flow on a thin vertical cylinder. Datta et al. [8] gave a non-similar solution of a steady incompressible boundary layer flow over a horizontal cylinder with non-uniform slot injection or suction.

In all the studies mentioned above, the thermal boundary condition at the solid surface was assumed to be an isothermal wall or a constant wall heat flux, and thus the interaction between the solid surface and its adjacent boundary layer was neglected. In many engineering systems, however, the effect of conduction within the solid wall is significant and must be taken into account. The issue of the coupled heat transfer process between solid body (conduction mechanism) and the fluid flow (convection mechanism) results in a conjugated heat transfer problem. Luikv [9] obtained an approximate solution of a laminar flow past a flat plate of a finite thickness with the assumption of a linear temperature distribution in the plate. Pozzi and Lupo [10, 11] have solved the coupling of conduction with convection in a plate duct and natural convection along a plate. Yu et al. [12] used an effective method to solve the conjugate heat transfer of conduction and forced convection along wedges and a rotating cone. Vynnycky et al. [13] provided a comprehensive account of two-dimensional forced convection flow over a slab of both finte length and thickness. Huang and Chen [14, 15] have studied a vertical thin circular pin fin in forced convection flow and mixed convection flow. Wang [16] looked into the problem of conjugated mixed convection-conduction flow from a vertical cylindrical fin to non-Newtonian fluids. Very recently, Jilani et al. [17] investigated conjugate heat transfer by forced convection over a vertical cylinder with heat generation. In the previous studies [9-17], the researchers dealing with conjugated problems focused on the fluid flowing over a solid cylinder. In this paper, the effect of coupling of conduction with mixed convection along a vertical slender hollow cylinder is analyzed. A conjugated heat transfer parameter is introduced to reflect the characteristics of the conjugate problem. Furthermore, a powerful coordinate transformation is proposed for the governing equations. The local heat transfer rate and the skin friction coefficient are presented to demonstrate the influences of the wall conduction, the buoyancy force, the transverse curvature and the Prandtl number.

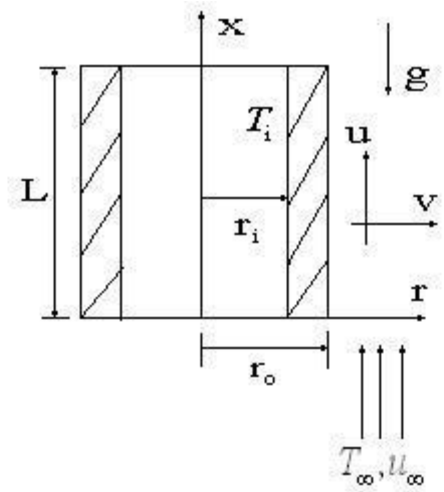

Fig.1 System schematics with coordinates

2. ANALYSIS

Consider a situation where a steady laminar flow of a Newtonian fluid passes a vertical slender hollow circular cylinder of length *L* and outer radius r_0 ($L >> r_0$). The system schematics and coordinates are depicted in Fig. 1. The gravitational acceleration acts in the downward direction. The velocity and temperature of the fluid at a distance remote from the cylinder are given by u_∞ and T_∞, respectively. The temperature of the inside surface of the cylinder is maintained at a constant temperature of T_i, where $T_i > T_\infty$. The fluid properties are considered to be constant except that density variations within the fluid are allowed to contribute to the buoyancy force.

Neglecting viscous dissipation and employing the Boussinesq approximation, the governing equations describing mass, momentum and energy conservation are

$$\frac{\partial}{\partial x}(ru)+\frac{\partial}{\partial r}(rv)=0 \qquad (1)$$

$$u\frac{\partial u}{\partial x}+v\frac{\partial u}{\partial r}=g\beta(T-T_{\infty})+\frac{\nu}{r}\frac{\partial}{\partial r}\left(r\frac{\partial u}{\partial r}\right) \qquad (2)$$

$$u\frac{\partial T}{\partial x}+v\frac{\partial T}{\partial r}=\frac{\alpha}{r}\frac{\partial}{\partial r}\left(r\frac{\partial T}{\partial r}\right) \qquad (3)$$

In the above equations, u and v are, respectively, the velocity components in the x and r directions, T is the temperature of the fluid, g is the gravitational acceleration, β is the thermal expansion coefficient, ν is the kinematic viscosity, and α is the thermal diffusivity. Equations (1) – (3) are subjected to the following boundary conditions:

at $r=r_0$: $u=v=0,\quad T=T_w(x)$ (4a)

as $r\to\infty$: $u=u_{\infty},\quad T=T_{\infty}$ (4b)

where subscripts w and ∞ refer to the wall and the boundary layer edge, respectively. Since $T_w(x)$ is the outer surface temperature of cylinder, which varies along the outer surface and depends on the flow dynamics and the solid conduction in the hollow cylinder. Therefore, an addition equation is required to determine the outer surface temperature of the slender hollow cylinder. Because the outer radius of the slender hollow cylinder, r_0, is small compared to its length, L, the axial conduction along the cylinder is negligible when compared with the radial conduction across the cylinder [11, 12, 13, 14]. The governing equation of conduction with slender hollow cylinder is shown below.

$$\frac{1}{r}\frac{\partial}{\partial r}\left(r\frac{\partial T_s}{\partial r}\right)=0;\quad 0\le x\le L,\quad r_i\le r\le r_0 \qquad (5)$$

The boundary conditions are

$$at\quad r=r_i:\quad T_s=T_i \qquad (6a)$$

$$at\quad r=r_0:\quad T_s=T_w(x),\quad -k_s\frac{\partial T_s}{\partial r}=-k_f\frac{\partial T}{\partial r} \qquad (6b)$$

where k_s and k_f are the thermal conductivity of the cylinder and the fluid respectively. The boundary conditions given in equation (6b) state the physical requirement that the temperature and heat flux of the cylinder and the fluid should be continuous across the solid-fluid interface. From equations (5), (6a) and (6b), the temperature distribution $T_w(x)$ at the interface is

$$T_w(x)=r_0\frac{k_f}{k_s}\ln\left(\frac{r_0}{r_i}\right)\frac{\partial T}{\partial r}\Big|_{r=r_0}+T_i \qquad (7)$$

To facilitate the numerical solution, the x-dependence of certain terms in the governing equations is reduced and the boundary conditions are simplified. This is accomplished by coordinate transformation based on a proper choice of transformation parameters [16]. The dimensionless parameters are

$$\xi=\frac{x}{L} \qquad (8)$$

$$\eta=\frac{r^2-r_0^2}{2r_0L}\left(\frac{\mathrm{Re}}{\xi}\right)^{1/2} \qquad (9)$$

$$\psi=r_0\alpha\,\mathrm{Re}^{1/2}\xi^{1/2}F(\xi,\eta) \qquad (10)$$

$$\theta=\frac{T-T_{\infty}}{T_i-T_{\infty}} \qquad (11)$$

where Re is the Reynolds number which is defined as

$$\mathrm{Re} = \frac{u_\infty L}{\nu} \qquad (12)$$

The stream function, ψ, automatically satisfies the continuity equation given in equation (1) with

$$u = \frac{1}{r}\frac{\partial \psi}{\partial r}; \quad v = -\frac{1}{r}\frac{\partial \psi}{\partial x} \qquad (13)$$

Substituting equations (8)-(11) into the governing momentum and energy equations yields

$$\Pr[\left(1+\varepsilon\eta\xi^{1/2}\right)F'']' + \frac{1}{2}FF'' + \xi\lambda \Pr^2 \theta$$

$$= \xi[F'\frac{\partial F'}{\partial \xi} - F''\frac{\partial F}{\partial \xi}] \qquad (14)$$

$$[\left(1+\varepsilon\eta\xi^{1/2}\right)\theta']' + \frac{1}{2}F\theta'$$

$$= \xi[F'\frac{\partial \theta}{\partial \xi} - \theta'\frac{\partial F}{\partial \xi}] \qquad (15)$$

The transformed boundary conditions are

$$F'(\xi,0) = 0; \quad F(\xi,0) = -2\xi\frac{\partial F}{\partial \xi}\Big|_{\eta=0};$$

$$\theta(\xi,0) = 1 + N_c\xi^{-1/2}\theta'(\xi,0) \qquad (16a)$$

$$F'(\xi,\infty) = \Pr; \quad \theta(\xi,\infty) = 0 \qquad (16b)$$

In the equations above, the primes indicate partial differentiation with respect to η. The new parameters in equations (14)-(16) are the Prandtl number

$$\Pr = \frac{\nu}{\alpha} \qquad (17)$$

the buoyancy parameter

$$\lambda = \frac{Gr}{\mathrm{Re}^2} \qquad (18)$$

with Grashof number $Gr = g\beta(T_i - T_\infty)L^3/\nu^2$.

the transverse parameter

$$\varepsilon = \frac{2L}{r_0 \mathrm{Re}^{1/2}} \qquad (19)$$

and the conjugate heat transfer parameter

$$N_c = \frac{r_0}{L}\frac{k_f}{k_s}\ln\left(\frac{r_0}{r_i}\right)\mathrm{Re}^{1/2} \qquad (20)$$

It should be noted that for the liming case of N_c=0, the thermal boundary condition in equation (16a) on the wall condition becomes isothermal, i.e. $\theta(\xi,0)=1$.

The physical quantities of special interest are the skin friction coefficient C_f and the number Nu. The two quantities are defined as

$$C_f = \frac{\tau_w}{\frac{1}{2}\rho u_\infty^2} \qquad (21)$$

and

$$Nu = \frac{hL}{k} \qquad (22)$$

From the definition of wall shear stress

$$\tau_w = \mu\frac{\partial u}{\partial r}\Big|_{r=r_0} \qquad (23)$$

a dimensionless skin friction group, SFG, can be formed as

$$SFG = \frac{1}{2}C_f \mathrm{Re}^{1/2} = \xi^{-1/2}F''(\xi,0)/\Pr \qquad (24)$$

Similarly, a dimensionless heat transfer group, HTG, can be formed as

$$HTG = Nu\,\mathrm{Re}^{-1/2}$$

$$= -\xi^{-1/2}\theta'(\xi,0)/\theta(\xi,0) \qquad (25)$$

3. NUMERICAL METHOD

The transformation of the governing equations reduces the numerical work significantly. The resulting system of coupled equations and associated boundary conditions are solved by an implicit finite difference technique. This technique is a modified version of the method described in Cebeci and Bradshaw [18].

The two-dimensional grid is nonuniform in order to accommodate the steep velocity and temperature gradient at the wall, particularly in the leading edge of the cylinder. The convergence criterion used was $\left|\left(\omega_{ij}^{k+1}-\omega_{ij}^{k}\right)/\omega_{ij}^{k+1}\right|_{\max}<10^{-4}$, where ω^k and ω^{k+1} are the values of the kth and (k+1)th iterations of F, F', F'', θ and θ'. The independence of the results from the mesh density has been successfully checked by trial and error.

4. RESULTS AND DISCUSSION

In order to verify the accuracy of the present computer simulation model, the results are compared with accepted data sets published in the open literature for the mixed convection of a Newtonian fluid flow along a vertical isothermal cylinder （$N_c=0$）with $\lambda=0$ and *Pr*=0.7. For different values of $\xi*$, the current results for the dimensionless liquid-solid interface heat transfer rate, $-\theta^{*'}(\xi*,0)$, and the skin friction factor, $F^{*''}(\xi*,0)$, are in a good agreement with those of [1], as shown in Table 1.

Table 1 Comparison of skin friction and local heat transfer rate with Pr=0.7, $\lambda=0$, $N_c=0$

$\xi^*=$	$F^{*''}(\xi^*,0)$		$-\theta^{*'}(\xi^*,0)$	
$\frac{4}{r_o}\left(\frac{\nu x}{u_\infty}\right)^{1/2}$	Chen [1]	Present results	Chen [1]	Present results
0.0	1.3282	1.3281	0.5854	0.5853
1.0	1.9172	1.9178	0.8669	0.8672
2.0	2.3981	2.3989	1.0968	1.0974
3.0	2.8270	2.8283	1.3021	1.3031
4.0	3.2235	3.2253	1.4921	1.4936

$F^{*''}(\xi^*,0)=4\times F''(\xi,0)/\Pr$;
$-\theta^{*'}(\xi^*,0)=-\theta'(\xi,0)\times 2$

Considering a hollow cylinder, the effect of the conjugated heat transfer parameter on the skin friction group (SFG) and the heat transfer group (HTG) are shown in Figs. 2a and 2b, respectively. The solid line and dashed lines in the figures correspond to the isothermal hollow cylinder ($N_c=0$) and the nonisothermal hollow cylinder ($N_c>0$) respectively. It can be seen that both of the SFG and HTG increase along the streamwise direction and decrease with the increasing values of N_c.This is because an increased value of N_c corresponds to a lower wall conduction and causes a reduction in the interfacial temperature. Furthermore, the decreasing interfacial temperature generates lesser buoyancy effects, and hence decreases the skin friction group and heat transfer group.

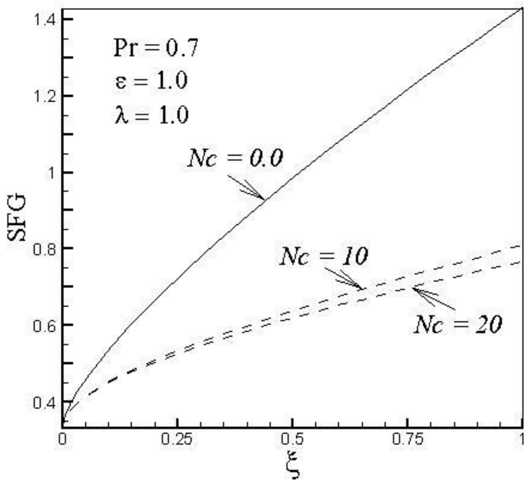

Fig.2a Effects of the conjugated heat transfer parameter on SFG

Fig. 3a and 3b plot the SFG and HTG distributions for different buoyancy parameters at Pr=0.7, ε=1.0 and $N_c=10$. It can be observed that the buoyancy effects in the mixed convection flow lead to acceleration of the fluid flow, which increases both of the local skin friction coefficient and heat transfer rate.

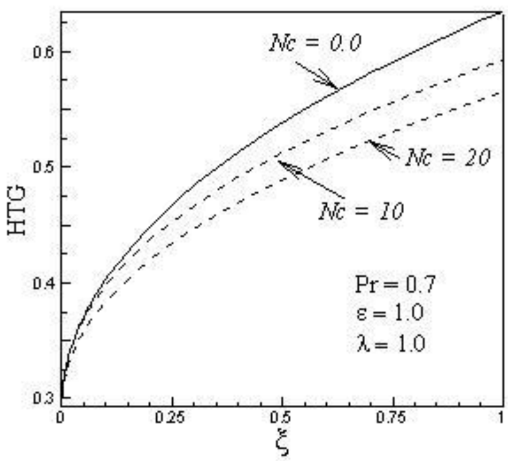

Fig.2b Effects of the conjugated heat transfer parameter on HTG

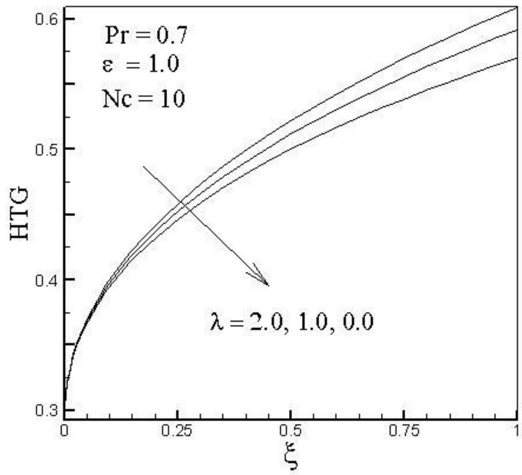

Fig.3b Effects of the buoyancy parameter on HTG

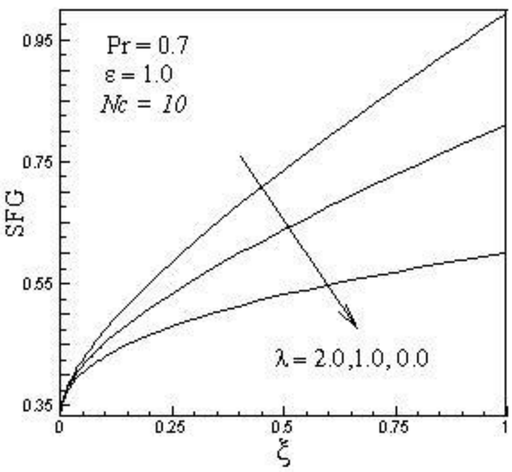

Fig.3a Effects of the buoyancy parameter on SFG

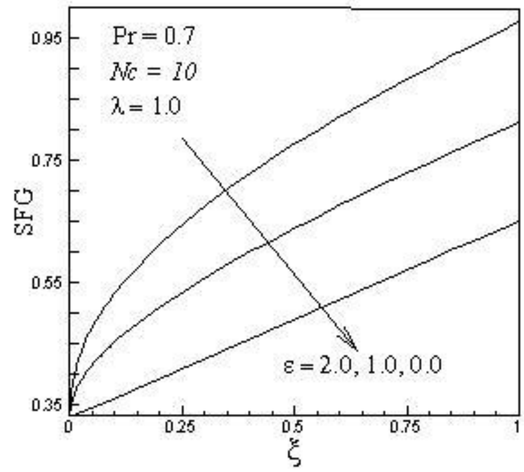

Fig.4a Effects of the curvature parameter on SFG

The variations of the SFG and HTG along the streamwise direction for various of the curvature parameter are presented in Fig. 4a and 4b respectively. For a given Pr, N_c and λ, the higher curvature parameter generates higher SFG and HTG values. The reason is that an increase of ε will produce favorable pressure gradients and hence cause an increase in SFG and HTG.

Fig. 5a and 5b respectively illustrate the variations of the SFG and HTG as a function of ξ, for selected values of the Prandtl number. As expected, an increase in Prandtl number Pr decreases the SFG and increases the HTG. The primary cause of this behavior is that higher values of Pr $\propto \nu/\alpha$ imply more viscous fluids, which reduced SFG. The opposite effect can be observed for HTG profiles that shift upward with higher Prandtl numbers, because Pr $\propto \nu/\alpha$ and fluids with smaller thermal diffusivities generate higher dimensionless temperature gradients at the wall. In addition, the effect of Pr on HTG is more significant than on SFG.

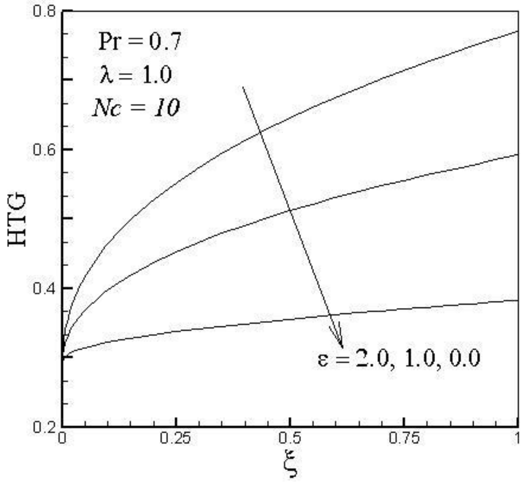

Fig.4b Effects of the curvature parameter on HTG

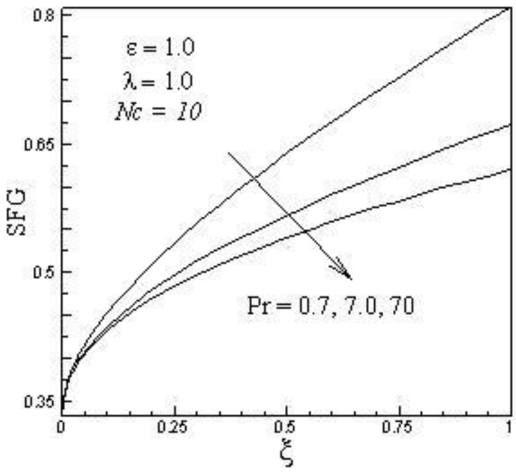

Fig.5a Effects of the curvature Prandtl number on SFG

5. CONCLUSIONS

An analysis of coupling conduction with mixed convection for Newtonian fluids along a vertical slender hollow cylinder has been presented. Numerical results of the transformed boundary layer equations have been obtained by using the implicit finite difference method. The results of computer experiments can be summarized as follows:

(1) The conjugated heat transfer parameter has a significantly influence on the fluid flow and heat transfer characteristics. An increase in the conjugated heat transfer parameter results in a reduction in the skin friction and the heat transfer.

(2) Both of the local skin friction coefficient and heat transfer rate increase with an increase in the buoyancy effect.

(3) The higher curvature parameter generates higher skin friction coefficient and heat transfer rate.

(4) An increase in Prandtl number decreases the skin friction coefficient and increases the heat transfer rate.

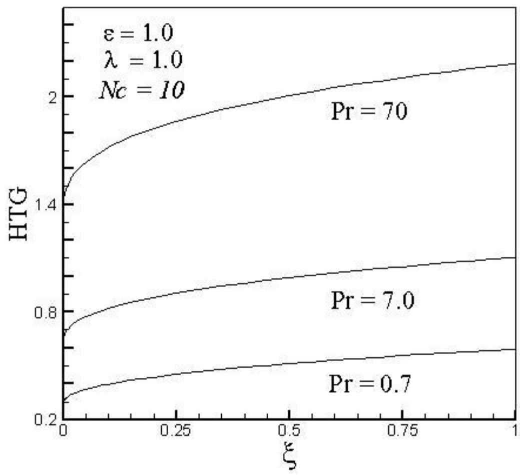

Fig.5b Effects of the curvature Prandtl number on HTG

REFERENCES

1. T.S. Chen and A. Mucoglu (1975), Buoyancy effects on forced convection along a vertical cylinder, J. Heat Transfer, Vol. 97, pp. 198-203.

2. A. Mucoglu and T. S. Chen (1976), Buoyancy effects on forced convection along a vertical cylinder with uniform surface heat flux, J. Heat Transfer, Vol. 98, pp. 523-525

3. M. N. Bui and T. Cebeci (1986), Combined free and forced convection in vertical slender

cylinders, J. Heat Transfer, Vol. 107, pp. 476-478.

4. S. L. Lee, T. S. Chen and B. F. Armaly (1986), Mixed convection along vertical cylinders and needles, Proc 8th In. Heat Transfer Conf., Vol.3, pp. 1425-1232.

5. S. L. Lee, T. S. Chen and B. F. Armaly (1987), Mixed convection along vertical cylinders and needles with uniform surface heat flux, J. Heat Transfer, Vol. 109, pp. 711-716.

6. T. Y. Wang and C. Kleinstreuer (1989), General analysis of steady laminar mixed convection heat transfer on vertical slender cylinder, J. Heat Transfer, Vol. 111, pp. 393-398.

7. M. Kumari and G. Nath (2004), Mixed convection boundary layer flow for a thin vertical cylinder with localized injection/suction and cooling/heating, Int. J. Heat Mass Transfer, Vol. 47, pp. 969-976.

8. P.Datta, D. Anilkumar and N. C. Mahanti (2006), Effect of non-uniform slot injection (suction) on a forced flow over a slender cylinder, Int. J. Heat Mass Transfer, Vol. 49, pp. 2366-2371.

9. A. V. Luikov (1974), Conjugate convection heat transfer problems, Int. J. Heat Mass Transfer, Vol.17, pp. 257-265.

10. A. Pozzi and M. Lupo (1988), The coupling of conduction with laminar natural convection along a flat plate, Int. J. Heat Mass Transfer, Vol. 31, pp. 1807-1811.

11. A. Pozzi and M. Lupo (1988), The coupling of conduction with forced convection in a plane duct, Int. J. Heat Mass Transfer, Vol. 32, pp. 1215-1221.

12. W. S. Yu, H. T. Lin and T. Y. Huang, (1991), Conjugate heat transfer of conduction and forced convection along wedges and a rotating cone, Int. J. Heat Mass Transfer, Vol. 34, pp. 2497-2507.

13. M. Vynnycky, S. Kimura, K. Kanev and I. Pop (1998), Forced convection heat transfer a flat plate: the conjugate problem, Int. J. Heat Mass Transfer, Vol. 41, pp. 45-59.

14. H. J. Hwang, C. C. Chen (1984), Vertical circular pin with conjugated forced convection-conduction flow, ASME J. Heat Transfer, Vol. 106, pp. 656-661.

15. H. J. Hwang, C. C. Chen (1985), Conjugate mixed convection and conduction heat transfer along a vertical circular pin, Int. J. Heat Mass Transfer, Vol. 28, pp. 523-529.

16. T. Y. Wang (1994), Conjugate mixed convection-conduction heat transfer along a vertical cylindrical fin in non-Newtonian fluids, Int. Comm. Heat Transfer, Vol. 21, pp. 383-396.

17. G. Jilani, S. Jayaraj and M. A. Ahmad (2002), Conjugate forced convection -conduction heat transfer analysis of a heat generating veruical cylinder, Int. J. Heat Mass Transfer, Vol. 45, pp. 331-341.

18. T. Cebeci and P. Bradshaw (1984), Physical and computational aspects of convection heat transfer, Springer -Verlag, New York.